Journal of Materials Processing Tech. 251 (2018) 146–159

Contents lists available at ScienceDirect

Journal of Materials Processing Tech.

journal homepage: www.elsevier.com/locate/jmatprotec

Influence of ultrasonic vibration on the plasticity of metals during compression process

Haiyang Zhou[a,b], Hongzhi Cui[a], Qing H. Qin[a,b,*]

[a] College of Civil Engineering, Shenzhen University, Shenzhen 518060, Guangdong, China
[b] Research School of Engineering, Australian National University, Canberra, ACT 2601, Australia

ARTICLE INFO

Keywords:
Ultrasonic vibration assisted compression
Aluminium
Titanium
Vibration frequency
Nanoindentation
EBSD

ABSTRACT

In this study, the influence of ultrasonic vibration on the plasticity of lightweight metals (aluminium and titanium) was investigated by means of ultrasonic assisted compression (UAC) experiments. The experiments were carried out based on the newly designed ultrasonic horns and transducers which can generate a series of vibration frequencies (20, 30 and 40 kHz) and adjustable vibration amplitudes (4.06–10.37 μm). It is found that, the ultrasonic vibration can reduce flow stress during UAC process for both aluminium and titanium, a phenomenon referred as ultrasonic softening effect. Different vibration amplitude and frequencies were specifically altered for observing the ultrasonic softening effect. The result is: in the range from 20 to 40 kHz the ultrasonic softening effect can be enhanced by increasing the vibration amplitude; however, increasing vibration frequency will decrease the ultrasonic softening effect, which is different from the previous acceptance stating that the vibration frequency (from 18 kHz to 80 kHz) has no influence on the ultrasonic softening effect. Apart from the ultrasonic softening effect, it is also found that the ultrasonic vibration can lead to residual hardening effect to aluminium and residual softening effect to the titanium. The influence of experiment parameters to the ultrasonic softening and residual effect during the UAC were assessed quantitatively and individually. These parameters include vibration frequency and amplitude, vibration duration as well as the sample size. Based on the UAC test within the elastic deformation stage, the mechanism of ultrasonic softening effect was explained from the occurrence of the unload phenomenon caused by ultrasonic vibration induced localized deformation. To validate the proposed mechanism, nanoindentation and electron backscatter diffraction (EBSD) test were carried out. According to the test result, ultrasonic vibration can induce plastic deformation and refine the grains for both aluminium and titanium sample. And for aluminium sample, comparing with the grains in the sample centre, the grains in the sample up boarder area are more sensitive to the ultrasonic vibration in terms of grain refinement, while for the titanium it is on the contrary.

1. Introduction

The ultrasonic vibration has been widely used as assistance to different metal processing technologies, such as ultrasonic metal welding, ultrasonic wire drawing, and ultrasonic assisted sheet forming. During the ultrasonic vibration assisted manufacturing, several parameters like vibration frequency, amplitude and duration of vibration are adjustable for different forming process and different materials.

In regard to the frequency influence on ultrasonic vibration assisted forming process, the first experimental study could be dated back to 1957, when Nevill and Brotzen (1957) conducted a tensile test of low carbon steel wire under superimposed ultrasonic vibration. By adjusting the length of wire, some longitudinal standing waves with a range of vibration frequencies were generated on the specimen wire. According to their report the stress reduction caused by the ultrasonic vibration is independent to the vibration frequency in the range from 15 kHz to 80 kHz. However, a concern is raised with the experiment setup used in this research. Although the frequency of input current can vary from 15 kHz to 80 kHz, the crystal and the exponential stub (also called as ultrasonic horn) were unchanged during the experiments. In this case a stable vibration mode of resonance could not be reached when the input frequency varies. Ideally with the change of input current, the crystal and exponential stub should be adapted according to the input frequency, so that the output vibration from the exponential stub to the specimen is controllable in the aspects of vibration amplitude and mode. Moreover, for studying the influence of vibration frequency on the plasticity of the sample, the length of the sample wire was adjusted to make it resonate to the exponential stub. This change however may

* Corresponding author: Tel.: +61 2 61258274; fax: +61 2 61255476.
E-mail address: qinghua.qin@anu.edu.au (Q.H. Qin).

http://dx.doi.org/10.1016/j.jmatprotec.2017.08.021
Received 30 November 2016; Received in revised form 2 August 2017; Accepted 16 August 2017
Available online 22 August 2017
0924-0136/

affect the plastic behaviour of the samples in vibration due to the size effect. Furthermore, during the tensile test, deformation of the sample may shift its natural frequency and even make it no longer resonates when the exponential stub keeps a same vibration mode as before. Blaha and Langenecker (1959) also reported that the reduced stress is independent to the vibration frequency when the frequency is from 15 Hz to 10^6 Hz. Their explanation was based on the fact that the vibration frequency in this range is much smaller than the natural resonant frequency of dislocation loops, which is normally 10^9 Hz. But no direct evidence was given to prove that without resonating with the dislocation loops the vibration frequency cannot influence the ultrasonic softening. These two reports have been cited by some studies to support the finite element modelling of the ultrasonic softening effect. Siddiq and El Sayed (2011) developed a crystal plasticity finite element model for the ultrasonic vibration assisted manufacturing process with considering the acoustic softening effect and they mentioned that the ultrasonic softening is independent to the vibration frequency in the range of 15–80 kHz. However during the calculation of the ultrasonic softening parameters, the velocity of the material point which is influenced by the vibration frequency was used. Djavanroodi et al. (2013) found that the forming force will be reduced by increasing ultrasonic vibration amplitude and frequency during equal channel angular pressing, and amplitude has more effective influence than frequency. Nevertheless, their conclusion was based on the finite element analysis and no experimental study about the influence of vibration frequency was conducted.

In the application of ultrasonic vibration, such as ultrasonic metal welding and ultrasonic assisted wire drawing, changing the height of a sample to make it resonate with the ultrasonic horn is not practicable. An alteration is to design the ultrasonic horn to let it match its resonance frequency to that of the ultrasonic transducer's, so as to achieve efficient input of the ultrasonic vibration power. For exploring the influence of ultrasonic vibration frequency to the plasticity of metals, in present study with changing the frequency of the input current (20, 30 and 40 kHz), three sets of experiment apparatuses featured with transducers and ultrasonic horns in different sizes are designed. These apparatuses can resonate with the input current at the frequency of 20 kHz, 30 kHz and 40 kHz, thus guarantee a stable and controllable vibration output. Details are illustrated in Section 2.

In addition to the vibration frequency, vibration amplitude is another key factor affecting plasticity of metal in ultrasonic vibration assisted manufacturing. Numerous studies have confirmed that the magnitude of stress reduction depends on the vibration amplitude. But for exact quantitative relationship between ultrasonic vibration amplitude and stress reduction, the answers were inconsistent. Siddiq and El Sayed (2012a) proposed a phenomenological crystal plasticity model of aluminium for the ultrasonic consolidation process. In this model the ultrasonic softening effect was suggested to be proportional to the acoustic intensity which is in turn proportional to the square of the amplitude accordingly. And in their following work, Siddiq and El Sayed (2012b) used the same equation to calculate the ultrasonic vibration induced softening effect, however with the use of different parameters the ultrasonic softening effect of aluminium was defined to have a quadratic relation with ultrasonic intensity. Although, both of these two works took aluminium as the subject, by using different sources of experimental data to do the equation fitting, different relationship between the ultrasonic softening and vibration amplitude were achieved. Huang et al. (2009) studied the ultrasonic wire bonding of copper, it showed that the reduction of stress of copper was proportional to the vibration amplitude. And by comparing the results of cooper and gold, they suggested that the ultrasonic softening may be largely influenced by the crystal structure rather than the materials type. Since titanium has a different crystal structure to aluminium and there is little quantitative research about the ultrasonic softening of titanium, so in this study through using of titanium samples which have a relatively high strength, the influence of vibration amplitude to the stress reduction during UAC has been studied over a wide range of amplitudes.

On the other hand, there have been some reports on the mechanism of the ultrasonic softening effect. Malygin (2000) proposed a stress superimposition mechanism for the acoustic plastic effect based on the computer simulation. However Daud et al. (2007) found that the oscillatory stress induced by the ultrasonic vibration was smaller than reduction of mean stress during the ultrasonic vibration assisted compression and tension test of aluminium. To better understand the underlying mechanism of acoustic plasticity from the microstructure aspect, Siu and Ngan (2011) conducted the dislocation dynamic simulation on the interaction of dislocations with the superimposing of quasi-static and oscillatory stress. They found that the dislocation annihilation was enhanced in this combined stress state and it led to larger strain at the same loading history. Furthermore, since ultrasonic vibration just works like an ultra-high frequency impacting in the UAC test, it is necessary to investigate if the strain induced by the ultrasonic vibration is localized or evenly distributed to have a better understanding of the ultrasonic softening effect.

Besides ultrasonic softening effect, the high frequency vibration could also cause the residual effect to the metal materials during plastic deformation. Yao et al. (2012) conducted the ultrasonic assisted compression test of aluminium and built a crystal plasticity based model for this process. In their research the acoustic residual hardening effect was interpreted by the multiplication of dislocation density which was time dependent, and the ultrasonic residual softening effect were also mentioned as the possible result of dislocation annihilation. Lum et al. (2009) found that during the ultrasonic wire bonding of gold there existed a residual softening effect. They explained that the ultrasonic vibration could induce sufficient heat input to the sample to make it annealed and reduce the dislocation; hence there was a residual softening effect. The same theory was also applied to the cooper, when Huang et al. (2009) studied the residual softening effect during the ultrasonic wire bonding of it. Zhou et al. (2017) conducted EBSD test to investigate the ultrasonic vibration induced residual effect of aluminium and titanium. They found that for aluminium the ultrasonic vibration reduced the grain size and changed the orientation of the grains, and both of which contribute to the residual hardening effect. However, for the titanium, the grain refinement induced by ultrasonic vibration is limited. And the ultrasonic vibration can promote the saturation of twinning and reduce the fraction of twinning boundaries. Since the twinning boundary works as a hardening factor to titanium, the UAC titanium sample exhibits a residual softening effect with less twinning boundaries. Although there have been some discussions about the mechanisms of the ultrasonic vibration induced residual effects, the quantitative relationship between the ultrasonic vibration parameters and the residual effects still needs to be investigated.

Although there have been many discussions regarding the influence of ultrasonic vibration parameters to the plasticity of metal, different conclusions have been drawn due to the differences in experiment apparatus applied among these studies. As shown in Table 1 in present study three ultrasonic vibration experiment setups with different vibration frequencies and adjustable amplitude were built to provide stable, adjustable and comparative parameters for the ultrasonic assisted compression test. Lightweight materials pure aluminium and titanium were chosen as samples due to their widely industrial usage and quite different crystal structures which may respond variously to the ultrasonic vibration. Comparing to previous studies, current work investigated the influence of ultrasonic vibration frequency and conducted microstructure analysis for the samples that subjected to transient ultrasonic vibration to study the mechanism of ultrasonic softening. What is more, the study of ultrasonic residual effects can give some hint in evaluating the service performance of the products manufactured with the assistance of ultrasonic vibration.

Table 1
Comparison between previous studies and present work about ultrasonic assisted processing.

Sources	Material	Methods	Conclusion
Gale E. Nevill (1957)	Steel	Varying sample length to adjust the vibration frequency.	Ultrasonic softening is frequency independent
Langenecker (1966)	Aluminium, Zinc, Steel	Increasing the ultrasonic intensity to change the vibration amplitude	Ultrasonic softening is proportional to square of vibration amplitude
Huang et al. (2009)	Cooper	Adjusting the horizontal vibration amplitude during the ball bonding	Ultrasonic softening is proportional to the vibration amplitude
This study	Aluminium, Titanium	Using three experiment setups with different vibration frequencies and amplitudes	Ultrasonic softening is influenced by frequency and is caused by the transient localized deformation of the sample.

2. Experimental

2.1. Materials

Commercially pure aluminium Al1060 and titanium ERTA1ELI were used in this study. The aluminium raw material was provided by SWA Co., Ltd. as annealed aluminium bar. The aluminium cylinder samples with a diameter of 4 mm were machined from the raw material. And there were 3 different heights for the aluminium samples: 2 mm, 4 mm and 8 mm. If not specified all the ultrasonic assisted compression tests of aluminium were carried out on the samples in 4 mm height. For the titanium, the raw material was from BAOTAI Co., Ltd., presented as annealed titanium bar. It was then machined into cylinder samples with a diameter of 2.4 mm and height of 2.4 mm. Both of the materials have already been annealed by the supplier, so no further heat treatment was conducted to the samples. The chemical compositions of the materials are presented in Table 2.

2.2. Ultrasonic assisted compression

The experiment setup for ultrasonic assisted compression (UAC) test is shown in Fig. 1(a). During the metal compression test conducted on the universal testing machine (Hualong-WDW300), the vertical ultrasonic vibration generated by ultrasonic transducer was applied directly to the samples from the ultrasonic horn. The compression experiment was controlled by the displacement of the cross head of the universal testing machine. For samples with different heights, the loading speed of the cross head was adjusted to provide a constant strain rate of $0.005s^{-1}$ to each sample. To investigate the influence of vibration frequency to the plasticity of metal during the UAC, three different vibration frequencies: 20.4 kHz, 30.8 kHz and 39.2 kHz were prepared (for the sake of expression convenience these vibration frequencies will be rounded off as 20 kHz, 30 kHz and 40 kHz respectively). As shown in Fig. 1(b), for each set of experiment apparatus, particular ultrasonic horn and transducer were applied to match their resonant frequency to frequency of the input current. When the ultrasonic vibration was applied to the sample, the load on the sample will drop immediately. Note that in this study, with the applied ultrasonic vibration, the load on both aluminium and titanium samples did not exceed 3000 N. Based on the method of Daud et al. (2007) the vibration amplitude on the surface of ultrasonic horn was measured by Doppler Vibro-meter (PSV-400) when a load of 3000 N was applied on the ultrasonic horn and no load was applied on the ultrasonic horn respectively. The relationship between the vibration amplitude and the input voltage of three experiment setups with different frequency and loading condition is shown in Fig. 2. To control the output amplitudes for comparative study, the ranges of input voltages used for 20 kHz, 30 kHz and 40 kHz experiment setups were 90–110 v, 90–220 v and 180–240 v respectively. In these voltage ranges as shown in Fig. 2, the input voltage and the output vibration amplitude for each experiment setup are almost in a linear relationship and the loading condition does not have much influence on the vibration amplitude. The average value of vibration amplitudes with and without loads will be used in the following sections. Before UAC experiments, several load train calibration tests were conducted by compressing test without samples, in order to exclude the influence of the deformation of experiment apparatus and guarantee the reliability of the results. During the experiment the ultrasonic vibration was directly applied to the samples without using lubricant on the contacting surface for the efficient input of ultrasonic vibration energy.

2.3. Transient UAC test

In order to study the ultrasonic softening mechanism it is necessary to separately investigate the influence of ultrasonic vibration on the material plasticity from the influence of normal compression, so a transient UAC experiment was carried out. In the experiment the transient ultrasonic vibration was applied to an aluminium sample with 8 mm height in the stage of elastic deformation. The 8 mm height aluminium sample was firstly compressed till the load reached 200 N, then this load was maintained by holding the crosshead. In this situation the average engineering stress in the sample was about 15.9 MPa and the deformation of the sample was elastic. Then a 20 kHz ultrasonic vibration with amplitude about 15.0 μm was applied to the sample, instantly the sample was completely unloaded.

Furthermore, to study the follow-up development of the immediately ultrasonic softening effect, a loading-transient vibrating-loading cycle experiment was carried out. First, a normal compression was applied to the titanium sample with a height of 2.4 mm. When the crosshead moved upward by 0.6 mm and the compression forced reached about 3800 N, a 30 kHz ultrasonic vibration with the amplitude of 10.37 μm was applied to the sample. The compressive force immediately dropped due to the applied ultrasonic vibration. When the load reached the lowest point, the ultrasonic vibration was stopped and then the load was increased to 3000 N by moving the crosshead upwards, followed through the ultrasonic vibration was applied to the sample again. This loading-transient vibrating-loading cycle was repeated several times to simulate the development of the ultrasonic softening effect.

Table 2
Chemical compositions of commercially pure aluminium Al1060 and titanium ERTA1ELI in wt.%.

Al1060(O3)	Al	Si < 0.25	Cu < 0.05	Mg < 0.05	Zn < 0.05	Mn < 0.05	Ti < 0.03	V < 0.05	Fe 0–0.40
ERTA1ELI(M)	Ti	Fe 0.02	C < 0.01	N < 0.01	H 0.02	O 0.08			

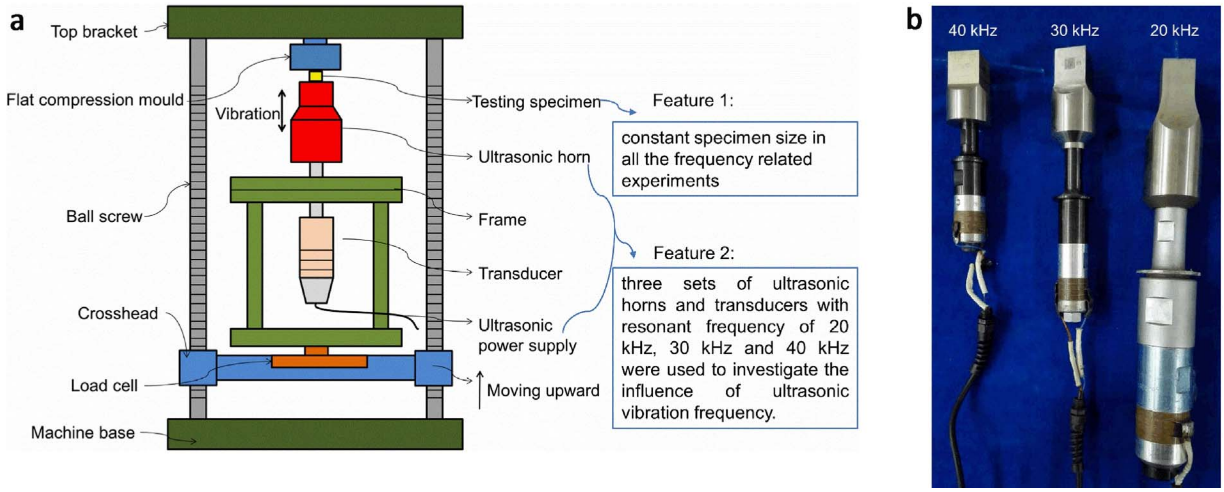

Fig. 1. (a) Schematic of experiment setup for ultrasonic vibration assisted compression test. (b) Ultrasonic horns and transducers for different frequencies.

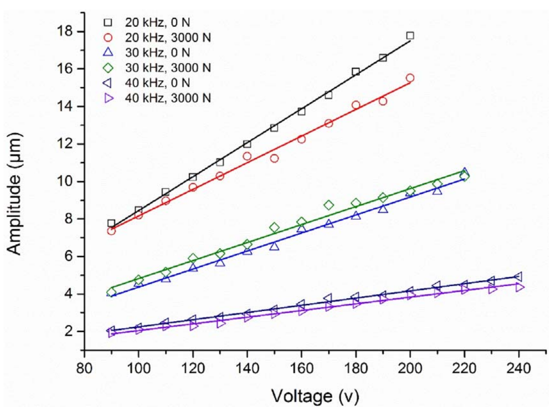

Fig. 2. Relationship between the input voltage and vibration amplitude in experiment setups with different frequencies and loading conditions.

2.4. Nanoindentation characterization

To study the transient UAC induced deformation to the sample as well as the ultrasonic softening mechanism, nanoindentation tests were conducted along the longitudinal axis of the aluminium and titanium samples. If the ultrasonic vibration induced certain deformation to the sample, due to the work hardening mechanism which involves dislocation tangles, grain refinement and residual stress, the ultrasonic vibration induced deformation could be characterized by the hardness distribution along the longitudinal axis of the samples.

As shown in Fig. 3, the original aluminium (4 mm in height) and titanium (2.4 mm in height) sample as well as the compressed and UAC sample were prepared for the nanoindentation tests. For both aluminium and titanium the compression sample was deformed to a strain of 15%. And for the UAC samples, they were first compressed to a strain of 15%, then a 30 kHz ultrasonic vibration was applied to the sample, for aluminium sample the amplitude was 4.65 μm while for titanium sample the applied amplitude was 10.37 μm. All these samples were first cut and mounted into resin and the gradually mechanically polished to a fine surface. The last polishing step was finished with 0.04 μm colloidal silica to reach a mirror like surface without polishing induced residual stress. Then the test was done on a TriboIndenter TI 900 Low-Load system along the axis of the sample from top surface to the bottom surface. The nanoindentation of aluminium sample was conducted with a load of 2 mN while the loading rate and unloading rate were both 2 mN/s. Similar nanoindentation tests were conducted on the titanium samples with a load of 5 mN and loading speed of 5 mN/s. For all the samples a step size of 5 μm was applied between two indents.

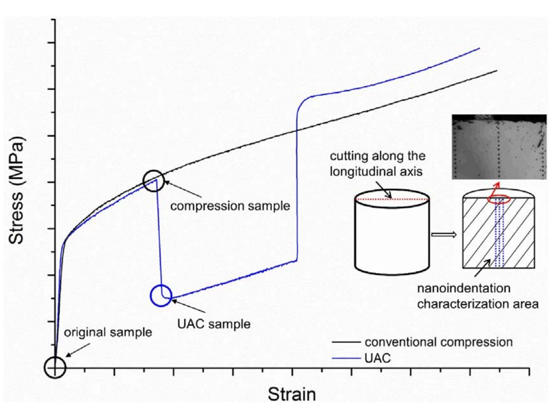

Fig. 3. Schematic drawing for the sample preparation for nanoindentation.

2.5. EBSD characterization

To understand the microstructure evolution induced by the ultrasonic vibration, as well as to further explore the ultrasonic softening mechanism from a microstructure point of view, the samples used in previous nanoindentation tests were re-polished to conduct the EBSD characterization for aluminium and titanium samples. For aluminium sample, it were first coarse polished with different grade diamond polishing solutions and then final polished with colloidal silica polishing solution for 40 min to remove the influence of previous nanoindents. And for titanium sample, after fine polishing with colloidal silica, a polishing solution consists of colloidal silica, hydrogen peroxide (30%), ammonia (28%) and DI water with a volume ratio of 8:1:1:10 was used to polish the sample for 10 min to improve the sample quality. The EBSD characterizations were conducted on Zeiss UltraPlus analytical FESEM (with Oxford HKL EBSD system) with a beam current of 4 nA, working distance of 24.5 mm and accelerating voltage of 20 kV for aluminium, 15 kV for titanium. For the original samples, a step size of 1 μm was used while for the deformed samples the step size used was 0.4 μm.

For the original sample EBSD mapping was only conducted in the centre of the sample due to its uniformly distributed microstructure. However the transient ultrasonic vibration may induce certain deformation to the sample can cause the non-uniform deformation within the sample. So for the compressed and UAC samples, the EBSD mapping area will be chosen based on the result of nanoindentation test, which

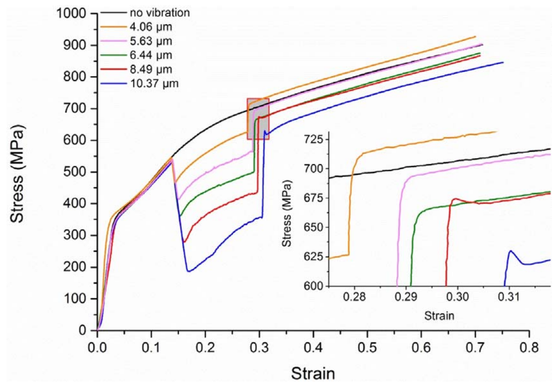

Fig. 4. Influence of amplitude to the plasticity of titanium during UAC with 30 kHz vibration.

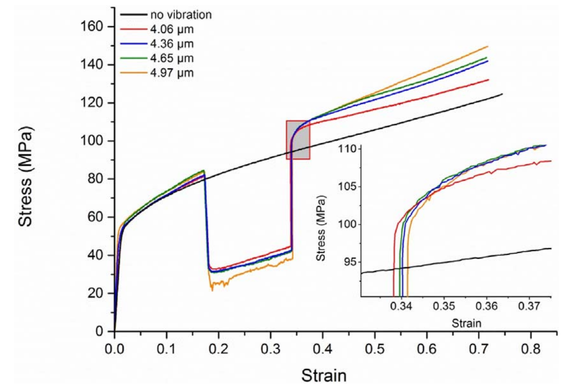

Fig. 5. Influence of amplitude to the plasticity of aluminium during UAC with 30 kHz vibration.

will be further illustrate in the following section.

3. Results and discussion

3.1. Influence of ultrasonic vibration to the plasticity of aluminium and titanium

The influence of ultrasonic vibration to the plasticity of aluminium and titanium during the UAC process is shown by the evolution of stress and strain curve.

(a) Influence of amplitude of ultrasonic vibration

As shown in Fig. 4, the titanium samples (2.4 mm in height) were firstly compressed to reach a strain of 0.14, and then the ultrasonic vibrations with a frequency of 30 kHz and different amplitudes were applied to the samples using the method shown in Fig. 1(a). When the ultrasonic vibration was superimposed to the sample, the stress dropped immediately with a slightly increase of strain. And with an increase in the vibration amplitude, the stress reduction was enhanced. This phenomenon is called ultrasonic softening effect. Under the largest vibration amplitude of 10.37 μm the stress is reduced by 66.3%. After the sample reached a strain around 0.3 the ultrasonic vibration stopped. In the following compression process the stress first increased linearly with the compression, indicating an elastic process and then turned into a plastic deformation process. When the vibration amplitude was at the smallest value of 4.06 μm after the vibration, the linearly increased stress surpassed the flow stress of the normal compression sample with the same strain. This reveals a residual hardening effect of ultrasonic vibration on the stress of the titanium. Nevertheless, with the increase of the vibration amplitude, the residual hardening effect turns to softening effect. And after being compressed with the assistance of 10.37 μm ultrasonic vibration, the stress of the titanium sample in the following compression process was 89.5% of the normal compression with the same strain of 0.31. When the applied vibration amplitude was above 8.49 μm, yield point occurred during the following compression process.

Similar to the titanium, the ultrasonic vibration caused an immediately stress reduction to aluminium sample (4 mm in height). As shown in Fig. 5, the maximum stress reduction was about 71.1% of the normal compression stress when a 4.97 μm and 30 kHz vibration was applied. Apart from the similar ultrasonic softening effect as titanium, the ultrasonic vibration induced quite different residual effect to aluminium, as only residual hardening was observed for aluminium sample. There was no yield point occurred during the following compression process for aluminium after the 30 kHz vibration, and the increased stresses with different vibration amplitudes were almost the same right after the vibration was stopped. With the compression going on, the sample that had been through UAC process with larger amplitude however achieved a more obvious hardening effect.

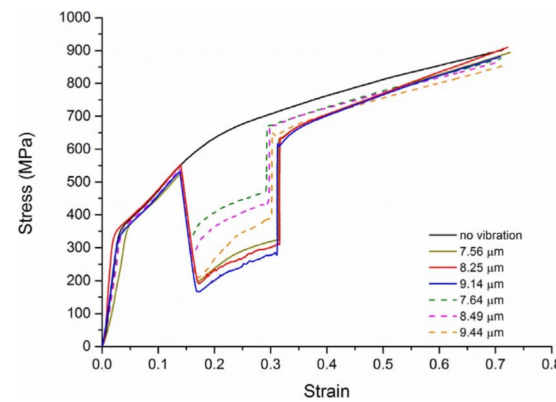

Fig. 6. Influence of frequency to the plasticity of titanium during UAC: comparison between 20 kHz (solid lines) and 30 kHz (dotted lines) vibrations with similar amplitudes.

(b) Influence of frequency of ultrasonic vibration

As shown in Fig. 6 to investigate the effect of vibration frequency to the plasticity of titanium, a comparison was made between the test results with 20 kHz and 30 kHz experiment setups. With similar vibration amplitudes, the ultrasonic softening effects from 20 kHz vibration are stronger than that from the 30 kHz vibration. In the following compression process right after ultrasonic vibration loading, the yield stress induced by 20 kHz vibration is lower than that by 30 kHz vibration. Moreover, the slope of the stress and strain curve for 20 kHz is larger than that for 30 kHz as well as that with no vibration.

As shown in Fig. 7 the influence of frequency to the plasticity of aluminium during UAC with 30 kHz and 40 kHz vibrations is similar to that of titanium samples which have been through 20 kHz and 30 kHz vibration. That indicates, under the same applied amplitude, lower frequency vibration can enhance the ultrasonic softening effect. And the residual hardening effect induced by 40 kHz vibration was weaker than that by 30 kHz vibration; nevertheless, obvious yielding phenomenon occurred after 40 kHz vibration.

(c) Influence of ultrasonic vibration duration

Fig. 8(a) and (b) demonstrate the influence of ultrasonic vibration duration (30 kHz) on the plasticity of titanium and aluminium during UAC process. For titanium as shown in Fig. 8(a), even a short time vibration can lead to the residual softening effect, however a short time (4 s and 12 s) ultrasonic vibration does not result in obvious yield point. Only after the vibration duration exceeds 24 s, the yield point occurs.

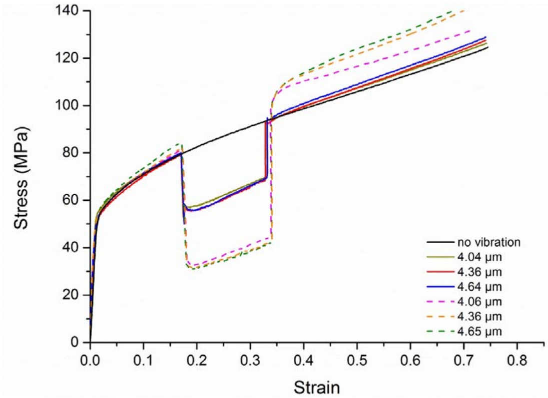

Fig. 7. Influence of frequency to the plasticity of aluminium during UAC: comparison between 30 kHz (dotted lines) and 40 kHz (solid lines) vibrations with similar amplitudes.

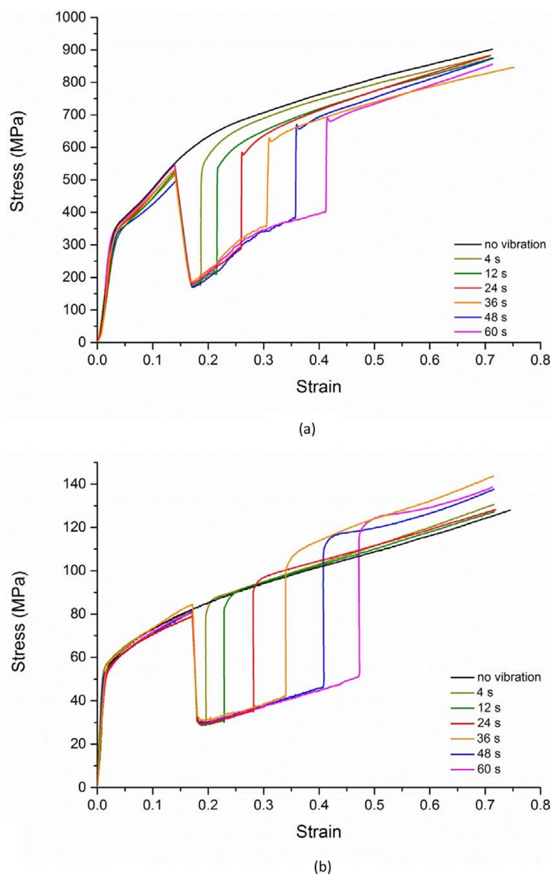

Fig. 8. Influence of ultrasonic vibration duration to the plasticity of (a) titanium with 30 kHz, 10.37 μm vibration (b) aluminium 30 kHz, 4.65 μm vibration.

And, for titanium the influence of vibration duration to the extent of the residual softening effect is not obvious. Nevertheless, as shown in Fig. 8(b) it is clear that the ultrasonic vibration duration would strengthen yield stress of aluminium due to the residual hardening effect.

(d) Influence of sample height

By applying the same vibration amplitude and frequency onto aluminium samples in different heights, the influence of sample height on the plasticity of aluminium during UAC was investigated. As shown in Fig. 9, due to the friction effect, the stress for the lower height sample was higher than the others'. When the ultrasonic vibration was applied,

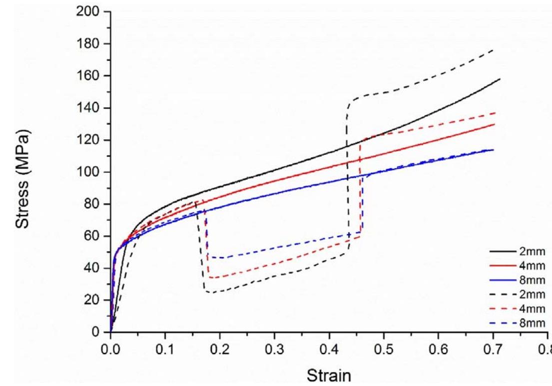

Fig. 9. Comparision of the influence of sample height to the plasticity of aluminium between normal compression (solid lines) and UAC process with 30 kHz and 4.06 μm vibration (dotted lines).

the stress reduction for the 2 mm sample was the highest which was about 69.1%. While the stress of the 4 mm sample and 8 mm sample reduced by 58.5% and 37.1% respectively. After the vibration was stopped, the stress increase for the 2 mm sample was higher than that of the 4 mm sample; while for the 8 mm sample, there was no obvious residual hardening effect at all.

3.2. Influence of experiment parameters to ultrasonic softening

In the work of Yao et al. (2012), Bagherzadeh and Abrinia (2015) the stress reduction was reported to be proportional to the vibration amplitude and the ultrasonic vibration induced flow stress reduction can be evaluated by the change of the non-dimensional stress ratio, which is given by:

$$\Delta\delta = \delta_u - \delta_0 = -\beta\left(\frac{U_E}{\hat{\tau}}\right)^{0.5} \tag{1}$$

where, β is the parameter found from experiment, the negative symbol represents that the stress will reduce due to ultrasonic vibration, $\hat{\tau}$ is the mechanical threshold which is related to the dislocation density and can be calculated for each strain based on the method showed in Yao et al. (2012) and U_E is the ultrasonic energy density of the sample written as

$$U_E = \rho\lambda^2\omega^2 \tag{2}$$

where, ρ is the density of the sample, λ and ω is the amplitude and angular frequency of the ultrasonic vibration respectively. According to Eqs. (1) and (2) the stress induced by the ultrasonic vibration is proportional to the product of vibration amplitude and vibration frequency. For a given experiment setup the vibration frequency is normally fixed, so the ultrasonic induced stress reduction is proportional to the vibration amplitude.

Also some study showed that the ultrasonic softening is in relation to the ultrasonic intensity (square of vibration amplitude). According to the report of Siddiq and El Sayed (2011) and Siddiq and El Sayed (2012b) the softening effect induced by the ultrasonic vibration is calculated by the ultrasonic softening term as

$$U_{soft} = (1 - dI_U)^e \tag{3}$$

where, d and e are ultrasonic softening exponent which can be found from experiment, and I_U is the ultrasonic intensity in the sample. According to Siddiq and El Sayed (2012b) the average of ultrasonic intensity in one cycle can be used to simplify the calculation, so I_U can be written as:

$$I_U = \frac{1}{2}\rho\omega^2\lambda^2 c \tag{4}$$

where, c is the sound velocity in the sample. For a given experiment

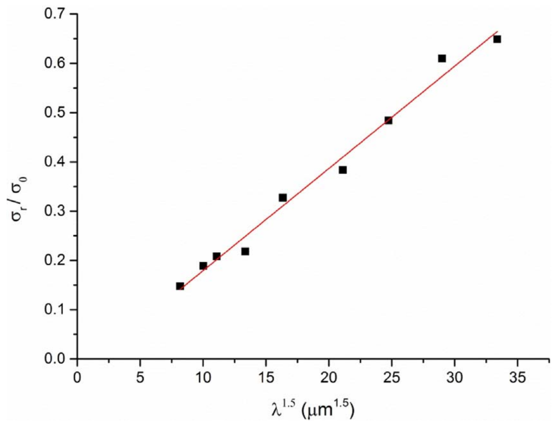

Fig. 10. Relationship between ultrasonic softening effect (σ_r/σ_0) and power of vibration amplitude $\lambda^{1.5}$ for titanium.

setup with a constant vibration frequency, when the value of e is taken as 1 (Siddiq and El Sayed, 2011, 2012a) the stress reduction is proportional to the square of ultrasonic amplitude and when e equals to 2 (Siddiq and El Sayed, 2012b) the stress reduction has a quadratic polynomial relationship with the square of ultrasonic amplitude.

Although the two different expressions discussed above give the relatively accurate descriptions of the relationship between the ultrasonic vibration induced stress reduction and the vibration amplitude, none of them covered the influence of vibration frequency and sample size.

In this study, the ratio of ultrasonic induced stress reduction and normal flow stress σ_r/σ_0 is used to characterize the ultrasonic softening effect. Based on the existing study mentioned above the ultrasonic softening is proportional to the m^{th} power of vibration amplitude λ, the value of m can be determined through linear fitting the experiment data. From the UAC test with different vibration amplitude of titanium samples, in this study m is taken as 1.5 and the relationship between the vibration amplitude and ultrasonic softening is shown in Fig. 10.

By calculating from the results on the influence of vibration frequency to the ultrasonic softening of titanium and aluminium, as shown in Figs. 6 and 7, the influence of vibration frequency to stress reduction ratio with different vibration amplitude is illustrated in Fig. 11.

From Fig. 11, it is found that for both aluminium and titanium samples with nearly the same vibration amplitude, a lower vibration frequency leads to a higher ultrasonic softening effect. It means the vibration frequency has a negative correlation to the ultrasonic softening effect in the range from 20 kHz to 40 kHz.

The influence of sample height to the ultrasonic softening effect is

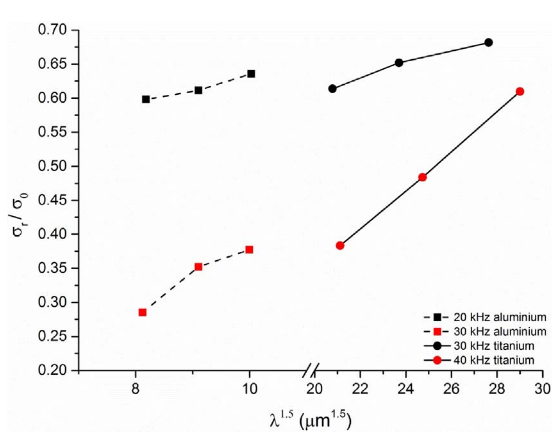

Fig. 11. Influence of vibration frequency to the ultrasonic softening effect: titanium sample under 20 kHz and 30 kHz vibration and aluminium sample under 30 kHz and 40 kHz vibration.

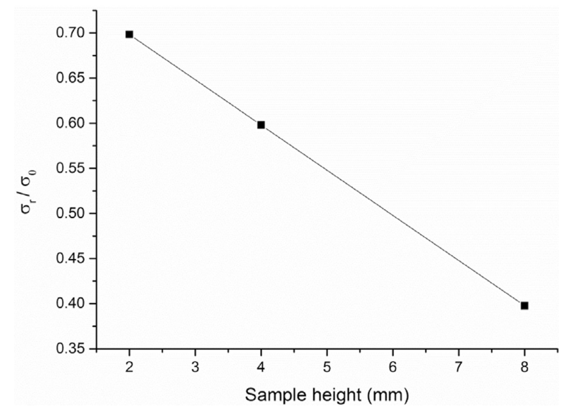

Fig. 12. Influence of sample height to the ultrasonic softening effect.

analysed based on the experiment data of aluminium presented in Fig. 9. As shown in Fig. 9 and 12, with the same ultrasonic vibration amplitude, the ultrasonic softening effect was reduced by increasing the sample height, and the stress reduction ratio has a linear relationship to the sample's height.

3.3. Ultrasonic residual effect

In the normal compression process after being subjected to the ultrasonic vibration, both the aluminium and titanium samples will yield again. The exhibited yield strength is different from the initial one and is also affected by the vibration parameters. In addition to the possible mechanisms of residual effect mentioned in the Introduction part, as shown in Figs. 6–8 the slopes of the strain and stress curves vary with applied vibration parameters. To better understand the influence of ultrasonic vibration to the plastic behaviour of aluminium and titanium during the follow-up compression process, the evolution of yield strength as well as strain hardening rate are investigated here. Since both pure aluminium and titanium do not have an obvious yield point during the normal compression process, the corresponding stress σ_0 with an offset strain of 0.2% after elastic deformation process will be used as the yield strength. The yield stress σ_Y after ultrasonic vibration is calculated in the same way. If yield points occur, the stress regarding to the lower yield point is used as yield stress. The yield stress reduction is calculated by

$$\sigma_{rY} = \sigma_Y - \sigma_f \tag{5}$$

where σ_f is the flow stress of the normal compression sample with the same strain as the UAC sample. The yield stress reduction ratio is given by σ_{rY}/σ_0.

And the strain hardening rate Θ is calculated by

$$\Theta = \frac{d\sigma}{d\varepsilon} \tag{6}$$

where σ and ε are respectively true stress and true strain. The calculation of strain hardening rate starts from the corresponding strain of yield strength.

(a) Residual hardening of aluminium

As shown in Fig. 13, the 30 kHz vibration leads to more severe residual hardening effect comparing to that of the 40 kHz vibration at the similar vibration amplitude. For each vibration frequency the residual hardening is enhanced by vibration amplitude. For 40 kHz test, the initial residual effect is softening effect due to the fact that ultrasonic vibration induced yield stress is smaller than the corresponding flow stress under the same strain. With the increase of vibration amplitude, a minor residual hardening effect occurs. The strain hardening rates of UAC samples in the follow-up compression process after ultrasonic

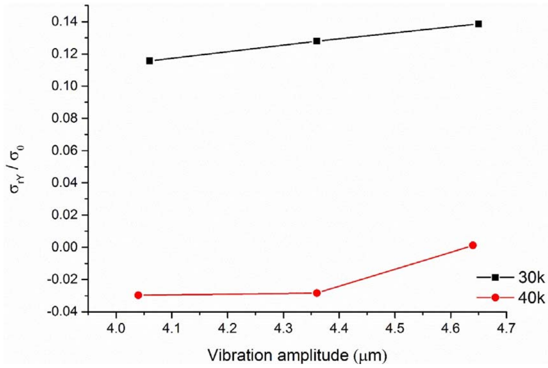

Fig. 13. Yield stress reduction ratio evolution with different vibration amplitude and frequency for aluminium samples.

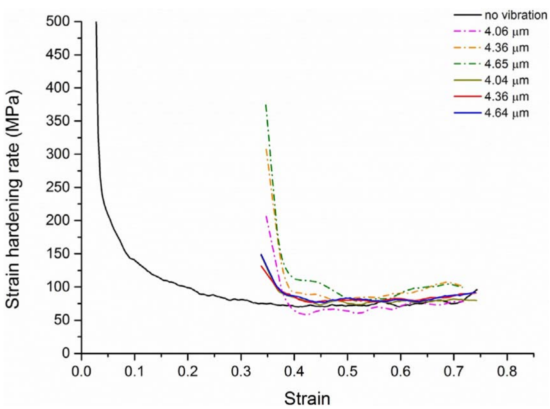

Fig. 14. Strain hardening rate evolution for 30 kHz (dotted line) and 40 kHz (solid line) vibration with different vibration amplitude for aluminium samples.

vibration are shown in Fig. 14. In most cases, the strain hardening rates of 30 kHz test are higher than that of the 40 kHz test, except the 30 kHz test with 4.06 μm vibration amplitude. And increasing the vibration amplitude can also increase the strain hardening rate.

For the 30 kHz tests, due to the gradual yielding phenomenon the calculated yield stress with 4–24 s vibration duration is below the corresponding flow stress during the normal compression test without applied vibration and under the same strain. As is shown in Fig. 15 the initial yield stress reduction ratio is negative. With the increasing of the vibration duration the residual effect turns to be hardening effect with a positive yield stress reduction ratio. Also as shown in Fig. 16, though the initial negative yield stress reduction ration indicates a residual softening effect, the strain hardening rate for UAC samples after being

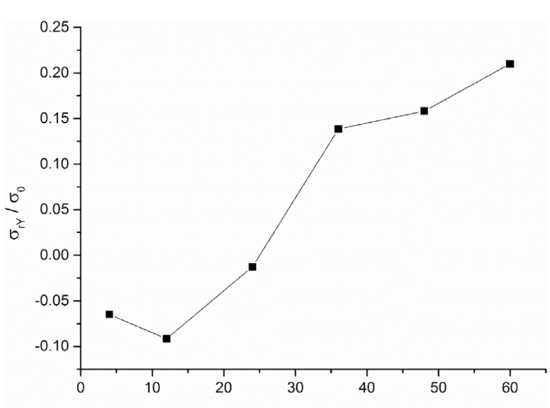

Fig. 15. Yield stress reduction ratio evolution with 30 kHz vibration and different vibration duration for aluminium samples.

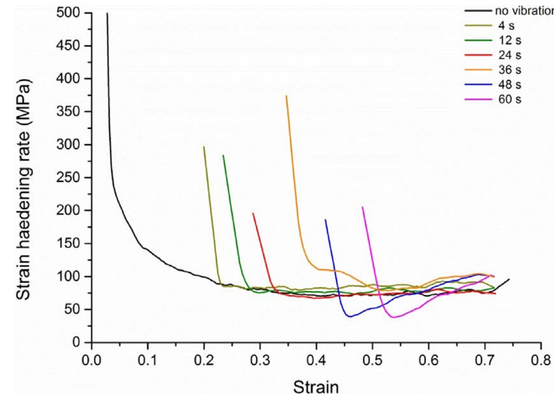

Fig. 16. Strain hardening rate evolution of aluminium samples with 30 kHz and 4.65 μm vibration for different vibration duration.

subjected to ultrasonic vibration is higher than that in the normal compression. Thus after the gradual yield phenomenon in the following compression process the samples exhibit residual hardening effect. It is also noticed that in Fig. 16, for the 48 and 60 s vibration test, the strain hardening rate first drops below that of compression test without vibration and then increases again. In generally, by applying longer vibration duration, a more severe residual hardening effect can be achieved.

(b) Residual softening of titanium

Titanium UAC sample shows a residual softening effect which reflects in Fig. 17 and Fig. 19 with a negative value of yield stress reduction ration. Similar to aluminium samples, the lower vibration frequency will lead to a more severe reduction of yield stress, and longer vibration duration can result in more residual softening effect. As for the strain hardening rate, from Fig. 18 it is obvious that ultrasonic vibration will induce a higher strain hardening rate for the titanium in the follow-up compression test. And the strain hardening rate of titanium after 20 kHz vibration is higher than that after 30 kHz vibration. Also in Fig. 20, it is found with longer vibration duration applied the higher strain hardening rate will be achieved.

3.4. Generation of ultrasonic softening

The transient UAC test was conducted to study the generation of ultrasonic softening effect. As shown in Fig. 21, the transient ultrasonic vibrated sample was compressed into a shape of reverse drum. In the work of Liu et al. (2013), a similar shape was formed during the ultrasonic vibrated compression test of a copper pin. They suggested that this reverse drum or umbrella shape of samples was caused by the high

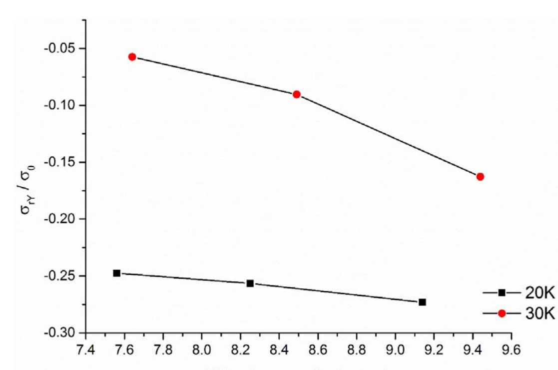

Fig. 17. Yield stress reduction ratio evolution with different vibration amplitude and frequency for titanium samples.

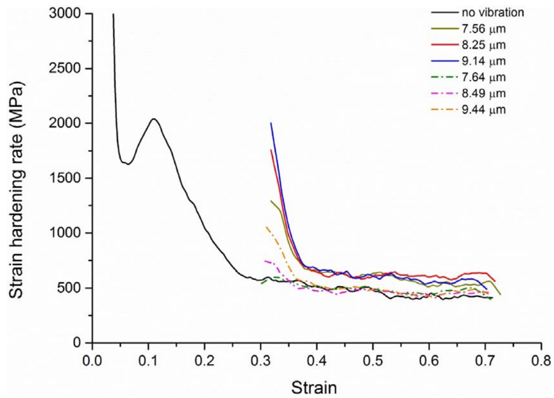

Fig. 18. Strain hardening rate evolution for 20 kHz (solid line) and 30 kHz (dotted line) vibration with different vibration amplitude for titanium samples.

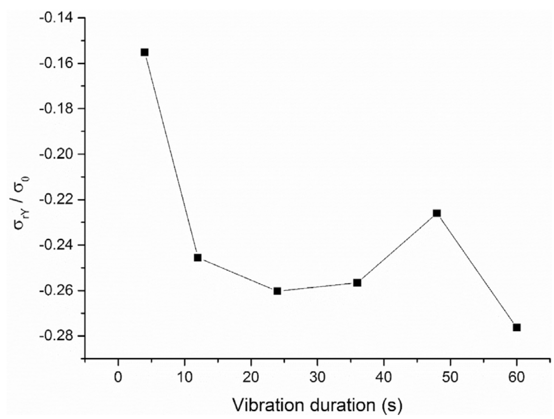

Fig. 19. Yield stress reduction ratio evolution of titanium samples in 30 kHz vibration with different vibration duration.

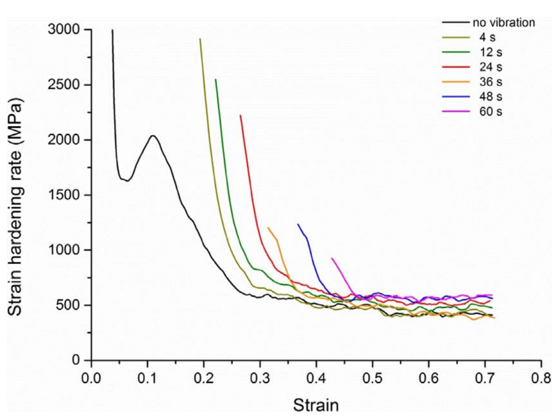

Fig. 20. Strain hardening rate evolution of titanium samples with 30 kHz and 10.37 μm vibration for different vibration duration.

velocity impacting according to the Taylor impact experiment (Wilkins and Guinan, 1973). During the impacting process, the stress at the impacting end of the sample exceeded the yield stress of the sample, and the plastic front caused by the impacting moved back to the elastic part of the sample. Meanwhile the elastic part of the sample would resistant to the plastic deformation, causing an umbrella shape at the end of the sample. Based on the discussion above, the unload phenomenon, i.e. ultrasonic softening effect is supposed to be caused by the localized plastic deformation induced by the ultrasonic vibration.

During the UAC process, the ultrasonic vibration works as high frequency impacting on the sample. It will induce the reduction of the sample's height, leading to an unload phenomenon from the crosshead

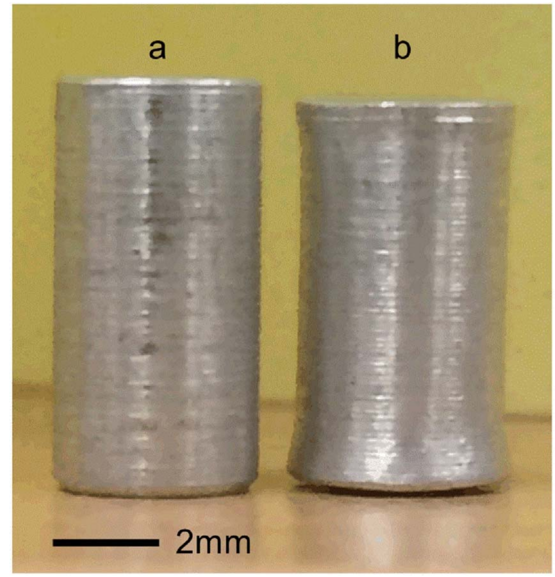

Fig. 21. Sample shape of a) first load to 200 N then unload to 0 N. b) first load to 200 N then apply ultrasonic vibration to the sample to make it unloads to 0 N.

to the sample. It should be noticed that, the ultrasonic vibration induced stress during one impact cycle time is very limited due to the small vibration amplitude, which is normally below the yield stress of the metal sample according to the work of Liu et al. (2012). Also the previous work of Daud et al. (2007) suggested that the ultrasonic vibration induced oscillatory stress was smaller than reduction of mean stress during the ultrasonic vibration assisted compression and tension test of aluminium, but the finite element model used in this work did not take the strain rate or microstructure evolution caused material property change into consideration. So the transient UAC test proved that different from the plastic deformation caused by high speed impact in Taylor impacting test, the ultrasonic vibration induced plastic deformation should be accomplished by the accumulation effect of several high frequency impact cycles in a short time. By applying higher vibration amplitude, the vibration induced deformation area is enhanced, and ultrasonic softening effect is improved. For the vibrations with same amplitude, a higher vibration frequency can accelerate the formation of localized plastic deformation, meanwhile the impact of higher vibration frequency will result in the material deforming at a higher strain rate. For aluminium and titanium with higher strain rate, the strength of the material will be improved with high strain rate deformation and the vibration induced deformation area tends to be more localized, leading weakened softening effect for the test with higher vibration frequency during UAC. As for the samples with different height, even if the vibration with the same amplitude will lead to the same localized deformation, the ratio of plastic deformation affected area to the sample height increases along with a decrease in the sample height. That suggests the localized deformation has more influence to the samples with lower height, hence the ultrasonic softening effect was more obvious for these samples.

3.5. Development of ultrasonic softening

The result of loading-transient vibrating experiment is shown in Fig. 22, with the repeat of the loading- transient vibrating-loading cycle, the softening effect was weakened (stage 1); this is thought to be caused by hardening effect due to the compression and ultrasonic vibration. After several cycles the ultrasonic vibration did not result in ultrasonic softening immediately. On the contrary, the applied ultrasonic vibration firstly increased the loading force by about 50 N, and then after several seconds of vibration the force dropped below 3000 N

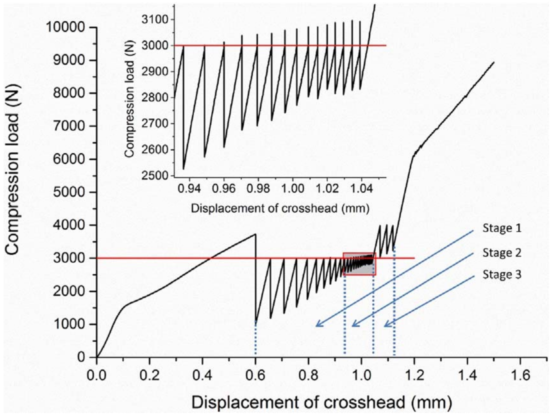

Fig. 22. Relationship between compression load and displacement in the loading- transient vibrating- loading cycle experiment.

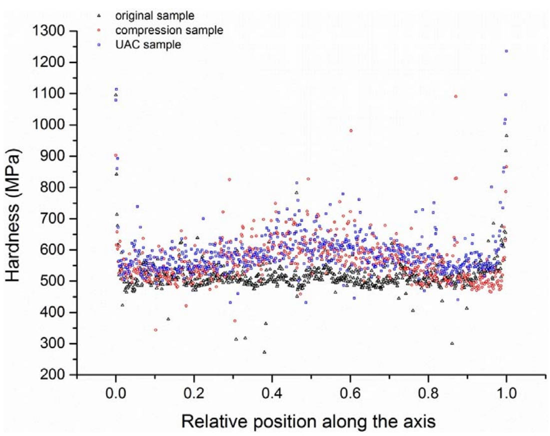

Fig. 23. Nanoindentation hardness distribution of aluminium sample along the longitudinal axis.

again (stage 2). This stage indicated that there was a balance between the work hardening and ultrasonic softening effect. And when the load was increased to about 4000 N (stage 3), the applied ultrasonic vibration induced obvious softening effect again. The development of the ultrasonic vibration can be summarised as follows: firstly, the ultrasonic vibration caused a softening effect on the deformed samples, and a balance between the work hardening and ultrasonic softening was reached, then the continued compression broke this balance and the ultrasonic vibration induced a softening effect again. With a high frequency ultrasonic vibration and low compression speed, the balance mentioned above can be reached in very short time, allowing the development of ultrasonic softening effect in a smooth way.

3.6. Sample deformation characterization by nanoindentation

The hardness distribution along the axis of all three aluminium samples was shown in Fig. 23, since the sample height is different before and after deformation, the relative position along the axis of each nanoindentation was used.

As shown in Fig. 23, the average hardness of the original sample is about 500 MPa. Since the sample was mechanically machined, so at both ends of the sample there is hardening layer, which is about 30 μm. After being compressed to a stain of 15%, the hardness distribution along the axis has a wave like shape. The hardness on the sample ends reduced a little bit compared with the original one, this is because the deformation induced material flow on the end surface. Then the deformation can break down the hardening layer and reduce the hardening by exposing fresh material to the sample end. Beneath the hardening layer, the sample hardness first dropped a little bit, from around 550 MPa to 500 MPa at a relative position of 0.15 and then increased to the maximum value at the centre of the sample, which is about 650 MPa. Comparing with the compressed sample, the hardness of the hardening layer of the UAC sample was increased with a maximum value about 1200 MPa. And the short time ultrasonic vibration increased the material hardness beneath the hardening layer. So the hardness of the UAC sample does not have the decline trend and it increased from 550 MPa (near the end) to 650 MPa (in the centre).

According to Fig. 23, it is obvious that the transient ultrasonic vibration can change the hardness of the sample along the longitudinal axis, but as for each sample there are over 650 nano-indents, it is difficult to make quantitative comparison between each sample. To make a more clear investigation, the relative frequency of different hardness value (with a bin size of 25 MPa) is presented in Fig. 24. It can be found that for the original sample the hardness value mostly distribute in the range of 490 MPa to 590 MPa (with a relative frequency over 0.025). And after the compression and UAC tests, for both deformed samples the curve of relative frequency shifts to the higher hardness value. For the compressed sample most of the hardness value ranges from 490 MPa to 690 MPa, while for the UAC sample the majority lies

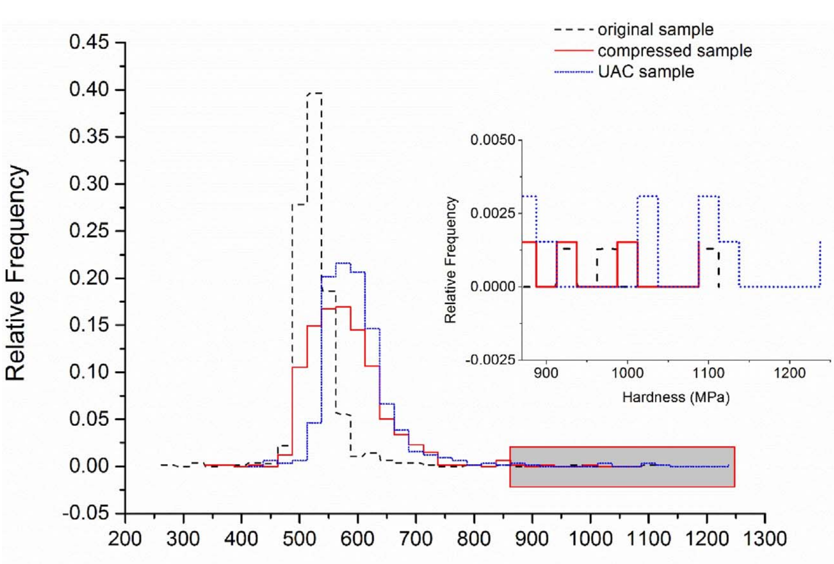

Fig. 24. The relative frequency of different hardness with a bin size of 25 MPa.

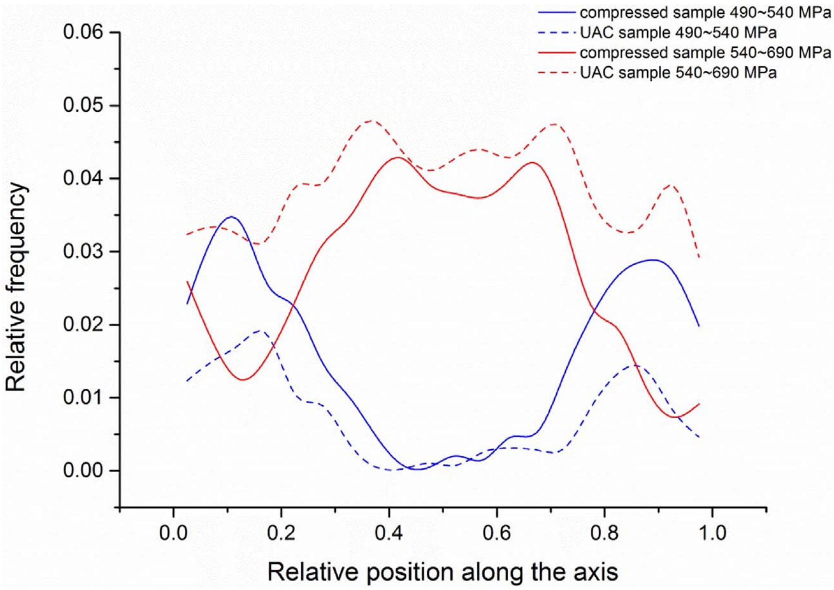

Fig. 25. The relative frequency of hardness in the range of 490–540 MPa and 540–690 MPa.

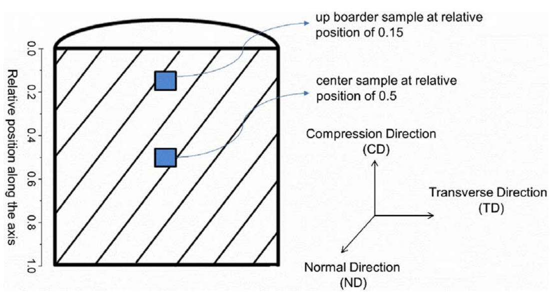

Fig. 26. Schematic drawing on the EBSD mapping area.

between 510 MPa to 690 MPa. Moreover the compressed sample has a higher relative frequency when the hardness is between 490 MPa and 540 MPa, while for the range from 540 MPa to 690 MPa the UAC sample has a higher frequency. As shown in Fig. 23 within the range of 490–540 MPa, for compressed and UAC samples the presented hardness concentrates on both ends of the sample. While for the hardness ranging from 540–690 MPa, it appears on the whole sample.

Fig. 25 shows the relative frequency of hardness along the longitudinal axis in the range of 490–690 MPa. In the range of 490–540 MPa, overall the compressed sample has a higher frequency than the UAC sample, while the UAC has a higher frequency than the compressed sample when the hardness varies from 540 to 690 MPa. However it is noticeable that the frequency difference mainly concentres in the sample ends area, when the relative position along the longitudinal axis ranging from 0.4to 0.7, the frequency are very close for the compressed and UAC sample.

According to the discussion above, it can be concluded that the transient ultrasonic vibration can not only induce a hardening layer to the sample ends, but also increase the hardness near the sample ends; meanwhile the hardness in sample centre area is less affected by the transient ultrasonic vibration. So it is confirmed that the transient ultrasonic vibration did induce plastic deformation to the aluminium and the induced deformation was not evenly distributed in the sample, the area near the sample ends was more affected.

The nanoindentation tests of titanium samples were also conducted, however comparing with the aluminium, titanium has less slip systems which make it more difficult to deform and the hardness of titanium is more sensitive to the grain orientations. So for the original undeformed sample the hardness is not consistent along the sample; and after being compressed and UAC process, the hardness of the samples still heavily fluctuated. In this research it is not practicable to use the hardness of titanium as an indicator of the deformation distribution of the sample.

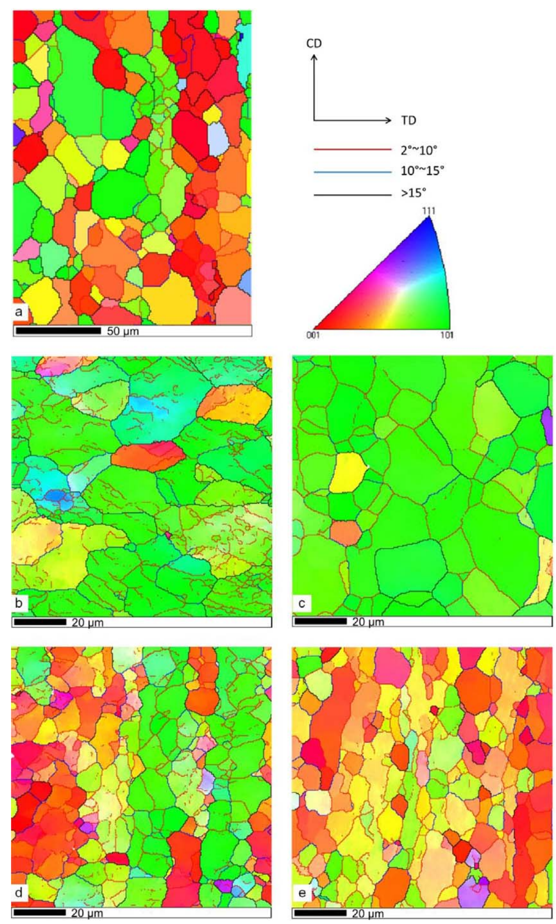

Fig. 27. Map of grain orientations as well as grain boundaries for (a) original sample (b) compression sample: centre (c) compression sample: up boarder (d) UAC sample: centre (e) UAC sample: up boarder.

3.7. Microstructure evolution characterized by EBSD

According to the nanoindentation test result, the EBSD

Table 3
Average distance between boundaries along compression and transverse directions.

Condition	d_{CD}(μm)	d_{TD}(μm)	d_{CD}/d_{TD}	$d_{CD}*d_{TD}$	f_{LAGB}
Original	11.89	9.68	1.23	115.10	1.68%
Compression (centre)	4.50	6.51	0.69	29.30	5.07%
Compression (up boarder)	9.79	9.67	1.01	94.67	2.37%
UAC (centre)	4.49	4.79	0.93	21.50	5.07%
UAC (up boarder)	6.38	4.85	1.32	30.94	4.50%

characterization was carried out on different areas of the compressed and UAC sample, as shown in Fig. 26.

(a) Microstructure evolution of aluminium

After the EBSD characterization the map of orientation with different grain boundaries was shown in Fig. 27. By using the line intercept method (30 lines per graph), the grain size of the samples was characterized by the average distance between grain boundaries with misorientation angle over 2 °, along both the compression (d_{CD}) and transverse directions (d_{TD}). According to the review of Lejček (2010), during the cold deformation, for the low angle grain boundary (LAGB), the tilt grain boundaries consist of edge dislocations, while twist grain boundaries are formed by an array of screw dislocations. So the dislocation evolution during UAC process can be evaluated by the change

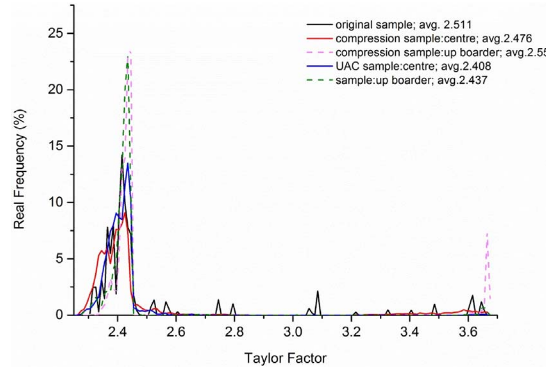

Fig. 29. Distribution of Taylor factors of EBSD samples.

of LAGB. To quantitatively study the change of LAGB during deformation, the area fraction of LAGB (f_{LAGB}) to the mapping area was calculated through dividing the pixels of LAGB by the entire pixels of the mapping. The value of f_{LAGB} could be influenced by different settings of the line width of grain boundaries, in this study the line width was set to 1 in the Channel 5 software. The statistical values are listed in Table 3.

As shown in Table 3, after the compression test, the value of d_{CD}, d_{TD} and their product are all smaller than the initial ones, so

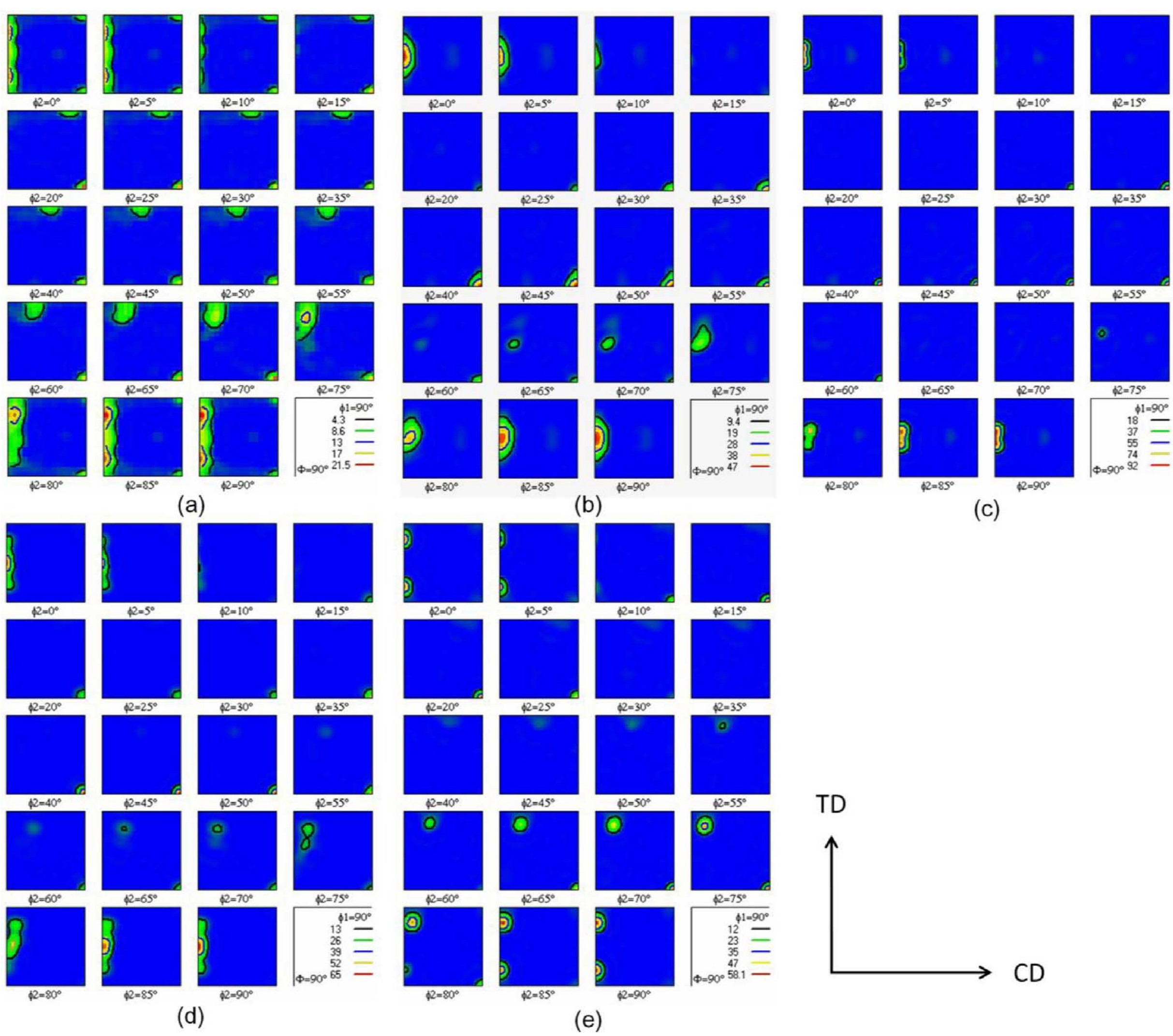

Fig. 28. Orientation distribution function of: (a) original sample (b) compression sample: centre (c) compression sample: up boarder (d) UAC sample: centre (e) UAC sample: up boarder.

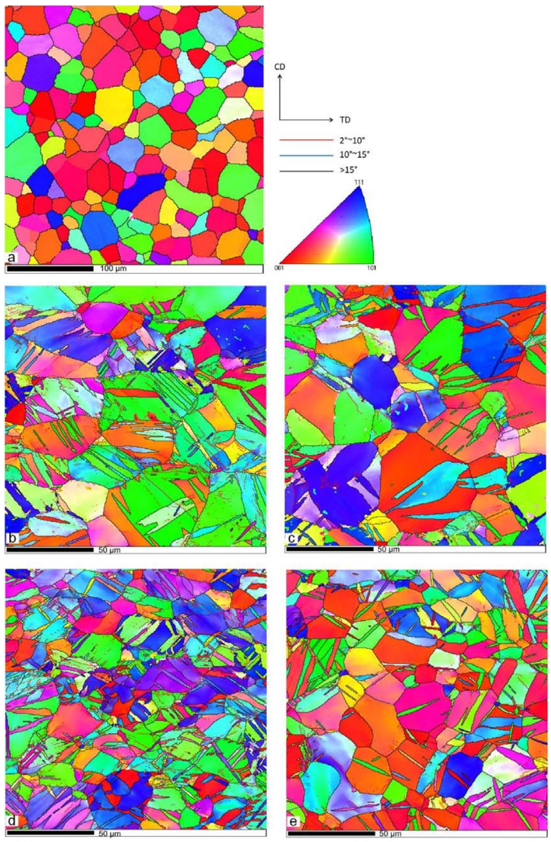

Fig. 30. Map of grain orientations as well as grain boundaries for (a) original sample (b) compression sample: centre (c) compression sample: up boarder (d) UAC sample: centre (e) UAC sample: up boarder.

Table 4
Average distance between boundaries along compression and transverse directions for titanium sample.

Condition	Angle (deg)	d_{CD}(μm)	d_{TD}(μm)	d_{CD}/d_{TD}	$d_{CD*}\ d_{TD}$
Initial	2	18.50	18.66	0.99	345.21
	15	19.93	19.53	1.02	389.23
Compression (centre)	2	3.05	4.47	0.68	13.63
	15	4.38	6.21	0.71	27.20
Compression (up boarder)	2	4.35	5.01	0.87	21.80
	15	5.53	6.23	0.89	34.45
UAC (centre)	2	2.25	3.04	0.74	6.85
	15	3.21	4.37	0.73	14.02
UAC (up boarder)	2	3.75	4.59	0.81	17.21
	15	4.63	5.40	0.86	25.00

compressive deformation reduced the grain size. And by applying the ultrasonic vibration these values are even smaller than the compression sample, so it is evidenced that the ultrasonic vibration can further refine the grains. What's more, by comparing the d_{CD}/d_{TD} and $d_{CD*}\ d_{TD}$ data from up boarder to centre of the compression sample, it is found that the deformation is more severe in the centre of the sample. For the compressed sample the $d_{CD*}\ d_{TD}$ value for up boarder is 3.2 times to the centre, while for the UAC sample it is only 1.40 times. Meanwhile the $d_{CD*}\ d_{TD}$ value in the centre of the compression sample is only 1.36 times of the UAC sample centre but for the up boarder the compression sample is 3.06 times to the UAC sample. So in terms of grain refining, the up boarder of the UAC sample is more sensitive to the ultrasonic vibration comparing to the centre of the sample and it is the reason why the nanoindentation result shows a localized deformation induced by ultrasonic vibration.

In this study, the grain refinement was achieved by the multiplication of LAGBs and the LAGBs can be used as an indicator of evolution of dislocations. By comparing the d_{CD} and d_{TD} value of compression and UAC samples, it is found that for the centre of the compression and UAC sample, the d_{CD} value is very close, but d_{TD} value of the compression sample is 1.36 times to the UAC sample. And for the up boarder area, the d_{TD} value of the compression sample is 1.99 times of the UAC sample while the d_{CD} value is 1.53 times of the UAC sample. This comparison indicates that for the UAC sample, there are more ultrasonic vibration induced LAGBs parallel to the compression direction than the transverse direction. And for the sample up boarder area the influence of ultrasonic vibration is more severe than the centre of the sample.

In the early work of Langenecker (1966), it was proposed that the ultrasonic vibration can increase the dislocation multiplication and prompt the mobility of dislocation. In the research of Liu et al. (2013), it is found that the ultrasonic vibration enhanced the movement of dislocation of cooper. From Table 3, the evolution of f_{LAGB} for the up boarder samples indicates that ultrasonic vibration increased the dislocation density. And as discussed above, the LAGBs formed by ultrasonic vibration induced dislocations tend to parallel to the compression direction which is also ultrasonic vibration direction.

From Fig. 27, it is found that the ultrasonic vibration not only refined the grains but also change the grain orientation. The orientation distribution function of EBSD samples is shown in Fig. 28. The original sample show a combination of fibre texture $<100>$ || CD, texture $\{013\}<100>$ and $\{013\}<\bar{1}00>$ and the maximum pole density occur on texture $\{013\}<100>$ which is 21.5. And after compression and UAC process, the centre and up boarder of compression sample as well as the centre of UAC sample, the maximum pole density occurs on a Goss texture $\{110\}<001>$. However for the UAC sample up boarder, there is no Goss texture and only the $\{013\}<100>$ and $\{013\}<\bar{1}00>$ texture with a maximum pole density of 58.1 were observed. So the applied transient ultrasonic vibration could cause the grain rotation to the up boarder area of the sample and changed its texture. For the UAC sample centre, it can be found that although it has a Goss texture, but it also tends to shift to the texture $\{013\}<100>$ and $\{013\}<\bar{1}00>$. So in terms of grain re-orientation the ultrasonic vibration has more influence to the sample up boarder area than to the centre.

The evolution of grain orientation during deformation will influence the activity of slip systems, and it can be characterized by Taylor factor. In Fig. 29 the distribution of Taylor factor with loading along the compression direction and its mean value are shown. Generally, lower value of Taylor factor indicates that the plastic deformation requires less slip shear strain and stress. So from the view of grain orientation,

Table 5
Area fraction of twinning boundaries to the mapping area.

Condition	$<11\bar{2}0>85°$	$<10\bar{1}0>64°$	$<\bar{1}2\bar{1}0>54°$	$<1\bar{1}00>35°$	LAGB
Compression (centre)	3.70%	0.81%	0.013%	0.0043%	3.19%
Compression (up boarder)	3.27%	0.094%	0.027%	0	1.75%
UAC (centre)	4.30%	1.88%	0.019%	0.019%	4.81%
UAC (up boarder)	3.33%	0.62%	0.037%	0.014%	1.73%

the activation of slip system is easier for the sample centre than the up boarder. And the ultrasonic vibration induced grain re-orientation reduced the Taylor factor of the UAC samples, especially for the up boarder area.

(b) Microstructure evolution of titanium

The grain orientation map with grian boundaries of titanium samples is shown in Fig. 30. Most of the grians in the original sample are equalized grains. Since the α phase titanium has a hexagonal close-packed (HCP) crystal structure, comparing with aluminium it has less slip systems. Except the slip and dislocation, the main deformation method for α titanum also includes twinning.

By line intercept method the grain size information is shown in Table 4. Since the deformation twinning will cause the grain refinement, so not only the grain boundaries over 2° but also the high angle grain boundaries (> 15°) were used to characterize the grain size.

As shown in 30 (b) and (c), after being compressed the titanium sample exhibitted lots of deformation twinnings and from Table 3 it is found that similar to the aluminium sample, the deformation of titanium is more severe in the centre of the sample. And comparing with Fig. 30(b) and (c)–(d) and (e), it is found that the ultrasonic vibraition induced more deformation twinnings and data in Table 3 shows the ultrasonic vibration further refined the grain size in the sample centre as well as the up boarder area.

To study the mechanism of ultrasonic vibraiton induced grain refinement, the area fraction of LAGB (f_{LAGB}) and twinning boundaries (f_{twin}) to the mapping area was calculated with the same method mentioned in aluminium sample analysis. The result is shown in Table 5.

As shown in Table 5, there are mainly two kinds of deformation twinning can be found in the sample: $\{10\bar{1}2\} < \bar{1}011 >$ tensile twinning with 85° misorientation angle and $\{11\bar{2}2\} < 11\bar{2}\bar{3} >$ compressive twinning with 64° misorientation angle. For both the compression and UAC sample, the sample centre has more twinning boundaries than the up boarder area. After being subjected to the ultrasonic vibration, the twinning in the sample increased comparing to the compression one, especially for the $\{11\bar{2}2\} < 11\bar{2}\bar{3} >$ compressive twinning. According to the research of Chichili et al. (1998), the twinning is easier to be triggered during high strain rate deformation. Due to the high frequency of ultrasonic vibration, the UAC sample was subjected to a transient higher strain rate deformation than the compression sample, leading to more twining boundaries. Also for the LAGB the UAC sample centre shows more LAGBs than the compression one, but as for the up boarder area, the fraction of LAGBs is close between the compression and UAC sample.

So for the titanium sample, the applied ultrasonic vibration increased the strain rate of deformation, induced more twinning as well as LAGB into the sample results a smaller grain size in the UAC sample. Different from the aluminium sample, the sample centre area is more sensitive to the ultrasonic vibration than the up boarder area. This can be evidenced by the fact that the ultrasonic vibration induced change of f_{twin} and f_{LAGB} is bigger for the sample centre than the up boarder area.

4. Conclusion

In this study three experiment apparatus that generate different vibration frequency were developed for the UAC test. Based on the results of our UAC test as well as the nanoindentation test and EBSD characterization, it is found that:

- The ultrasonic vibration can induce softening effect to both aluminium and titanium samples. The ultrasonic softening effect is affected by not only the ultrasonic vibration amplitude but also the vibration frequency. Specifically, in the range from 20 kHz to 40 kHz under the same vibration amplitude, lower vibration frequency can lead to stronger ultrasonic softening effect. The ultrasonic softening effect is also affected sensitively by the size of sample.
- The transient ultrasonic vibration increase the LAGBs in the aluminium samples and the induced LAGB tend to be parallel to the vibration direction. For titanium sample, the transient ultrasonic vibration increased both the fraction of LAGB and the twinning boundaries.
- For the aluminium sample, comparing to sample centre, the up boarder area of the sample is more sensitive to the influence of ultrasonic vibration. While for titanium sample, the ultrasonic vibration mainly affects the sample centre area.
- The mechanism of ultrasonic softening effect lies in the fact that the ultrasonic vibration acts like high frequency impacting to the samples, refines the grain size in the sample and leading to localized plastic deformation which causes an unload phenomenon.
- The residual effect caused by ultrasonic vibration is quite contrary between aluminium and titanium: residual hardening for aluminium and residual softening for titanium. The residual yield stress and strain hardening rate is also sensitive to the vibration amplitude, frequency, as well as the vibration duration.

Acknowledgement

Financial supports from the Automotive Australia 2020 CRC and Australian Research Council (Grant No. LP130101001) are fully acknowledged. The authors also greatly appreciate Dr. Hua Chen (Centre for Advanced Microscopy of Australian National University) for his help with the EBSD characterization and Mr. Sherman Wong (Department of Electronic Materials Engineering, Australian National University) for his help with the nanoindentation test.

References

Bagherzadeh, S., Abrinia, K., 2015. Effect of ultrasonic vibration on compression behavior and microstructural characteristics of commercially pure aluminum. J. Mater. Eng. Perform. 24, 4364–4376.
Blaha, F., Langenecker, B., 1959. Plastizitätsuntersuchungen von metallkristallen in ultraschallfeld. Acta Metall. 7, 93–100.
Chichili, D., Ramesh, K., Hemker, K., 1998. The high-strain-rate response of alpha-titanium: experiments, deformation mechanisms and modeling. Acta Mater. 46, 1025–1043.
Daud, Y., Lucas, M., Huang, Z., 2007. Modelling the effects of superimposed ultrasonic vibrations on tension and compression tests of aluminium. J. Mater. Process. Technol. 186, 179–190.
Djavanroodi, F., Ahmadian, H., Koohkan, K., Naseri, R., 2013. Ultrasonic assisted-ECAP. Ultrasonics 53, 1089–1096.
Nevill, Gale E., J.F.R.B, 1957. The effect of vibrations on the static yield strength of a low-carbon steel. ASTM Proc. 57, 751–758.
Huang, H., Pequegnat, A., Chang, B., Mayer, M., Du, D., Zhou, Y., 2009. Influence of superimposed ultrasound on deformability of Cu. J. Appl. Phys. 106, 113514.
Langenecker, B., 1966. Effects of ultrasound on deformation characteristics of metals. IEEE Trans. Sonics Ultrasonics 13, 1–8.
Lejček, P., 2010. Grain boundaries: description, structure and thermodynamics. Grain Boundary Segreg. Metals 5–24.
Liu, Y., Han, Q., Hua, L., 2012. Finite element simulation analysis of the ultrasonic vibration forging of an aluminum cylinder workpiece. Light Met. 257–264.
Liu, Y., Suslov, S., Han, Q., Hua, L., Xu, C., 2013. Comparison between ultrasonic vibration-assisted upsetting and conventional upsetting. Metall. Mater. Trans. A 44, 3232–3244.
Lum, I., Huang, H., Chang, B., Mayer, M., Du, D., Zhou, Y., 2009. Effects of superimposed ultrasound on deformation of gold. J. Appl. Phys. 105, 024905.
Malygin, G., 2000. Acoustoplastic effect and the stress superimposition mechanism. Phys. Solid State 42, 72–78.
Siddiq, A., El Sayed, T., 2011. Acoustic softening in metals during ultrasonic assisted deformation via CP-FEM. Mater. Lett. 65, 356–359.
Siddiq, A., El Sayed, T., 2012a. A thermomechanical crystal plasticity constitutive model for ultrasonic consolidation. Comput. Mater. Sci 51, 241–251.
Siddiq, A., El Sayed, T., 2012b. Ultrasonic-assisted manufacturing processes: variational model and numerical simulations. Ultrasonics 52, 521–529.
Siu, K., Ngan, A., 2011. Understanding acoustoplasticity through dislocation dynamics simulations. Philos. Mag. 91, 4367–4387.
Wilkins, M.L., Guinan, M.W., 1973. Impact of cylinders on a rigid boundary. J. Appl. Phys. 44, 1200–1206.
Yao, Z., Kim, G.-Y., Wang, Z., Faidley, L., Zou, Q., Mei, D., Chen, Z., 2012. Acoustic softening and residual hardening in aluminum: modeling and experiments. Int. J. Plast. 39, 75–87.
Zhou, H., Cui, H., Qin, Q.-H., Wang, H., Shen, Y., 2017. A comparative study of mechanical and microstructural characteristics of aluminium and titanium undergoing ultrasonic assisted compression testing. Mater. Sci. Eng.: A 682, 376–388.